Effect of tubulin diffusion on polymerization of microtubules

P. A. Deymier,[1] Y. Yang,[1] and J. Hoying[2]
[1]*Department of Materials Science and Engineering, The University of Arizona, Tucson, Arizona 85721, USA*
[2]*Biomedical Engineering Program, The University of Arizona, Tucson, Arizona 85721, USA*
(Received 7 January 2005; revised manuscript received 2 May 2005; published 19 August 2005)

The dynamics of microtubules (MT's) growing from a nucleation center is simulated with a kinetic Monte Carlo model that includes tubulin diffusion. In the limit of fast diffusion (homogeneous tubulin concentration), MT growth is synchronous and bounded. The microtubules form an aster with a monotonously decreasing long-time distribution of lengths. Slow tubulin diffusion leads to rapid dephasing in the growth dynamics, unbounded growth of some MT's, spatial inhomogeneities, and morphological change toward a morphology with bounded short MT's located in the nucleation center and unbounded long MT's with narrowly distributed lengths. The transition from unbounded to bounded growth is driven by the competition between the reaction rate of the tubulin assembly and the tubulin's diffusion rate. While the present study reports the effect of the tubulin diffusion coefficient on the transition, the results of the simulations are qualitatively comparable to the morphological and dynamical changes of centrosome-nucleated MT's from interphase to mitosis in cellular systems where the transition is regulated by the reaction rates.

DOI: 10.1103/PhysRevE.72.021906 PACS number(s): 87.16.Ka, 87.16.Ac

I. INTRODUCTION

Microtubules (MT's) are naturally formed proteinaceous tubular structures, 24 nm in diameter and up to many microns in length. MT's are biopolymers assembled from two related protein monomers α- and β-tubulins. In the presence of the small molecule guanosine triphosphate (GTP), these tubulin monomers form a GTP-liganded tubulin heterodimers (Tu-GTP), which will self-assemble into the MT structure. A MT consists of a two-dimensional helical lattice composed of 13 tubulin heterodimer protofilaments along the principal axis of the MT. Due to the geometry of self-assembly and differences in addition rates, a MT is polarized containing (−) and (+) ends. The (−) end contains an exposed α-tubulin and undergoes slower rates of heterodimer addition or substraction than the (+) end, which consists of an exposed β-tubulin [1,2]. Microtubules generated from pure tubulin exist in a dynamic state with net addition of monomers to the (+) end and net removal of monomers from the (−) end [3]. In the cell, self-assembly into the MT begins with nucleation taking place within a microtubule-organizing center involving a third monomer called γ-tubulin. *In vitro* experiments show that the protein γ-tubulin forms a ring complex (RC) that can directly nucleate microtubule assembly. γ-tubulin RC caps the (−) end of a microtubule and plays a key role in directing MT assembly [4,5]. In the test tube, nucleation complexes, termed nucleation seeds, can be prepared and can be used as organizing centers for subsequent MT polymerization [3]. Dynamic instability is an intrinsic property of MT's [6]. For tubulin concentrations above a critical value C_c, tubulin dimers polymerize into MT's, while below C_c, MT's depolymerize [7]. Near C_c, MT's exhibit dynamic instability during which an individual MT undergoes apparently random successive periods of disassembly (catastrophe) and assembly (rescue). The mechanism for transitions between a growing state and a shrinking state is generally believed to be associated with hydrolysis of bound GTP when tubulin heterodimers become incorporated within the microtubule lattice. Tu-GTP embedded within the lattice of the microtubule hydrolyses to guanosine diphosphate (GDP)-liganded tubulin (Tu-GDP). A growing microtubule is thus composed of a Tu-GTP cap of newly added Tu-GTP heterodimers and a core of Tu-GDP. Several theoretical studies have provided support for a cap model of MT dynamical instability. These studies include large cap models [8–12] and caps composed of a single layer of Tu-GTP [13–16]. Another aspect of dynamic instability appears in the existence of persistent oscillations in the mass concentration of microtubules [17]. At high Tu-GTP concentrations, many MT's are nucleated and grown. As MT's polymerize, the concentration of free Tu-GTP decreases and may reach a value below the critical concentration at which the MT's will transition to a depolymerizing state. The oscillations have been explained as resulting from the time lag between the depolymerization of MT's (i.e., solvation of Tu-GDP) and the exchange of GTP in the solution with liganded GDP to restitute free Tu-GTP, which can lead to a new phase of polymerization. Numerous models have been developed to simulate the collective oscillations of microtubules [17–22] and unraveled different types of growth depending on the initial concentration of tubulin and the restitution rate of Tu-GTP [19]. The majority of existing models is based on mean-field approaches and has assumed homogeneity of the tubulin heterodimer concentration. However, it has been noticed that dephasing of the oscillations in different regions and pattern formation may occur when the mean spacing between MT's is shorter than the diffusion length of free tubulin [19,23]. Diffusion of tubulin monomers has also been shown to play a role in MT organization. MT preparations self-organize spontaneously by reaction-diffusion processes [24–27]. For instance, *in vivo* and *in vitro* pattern formation develops in response to a competition between the reaction-controlled dynamics of MT assembly and disassembly and the diffusion of tubulin. For instance, as MT's grow from their plus end and disassemble from their minus end, MT

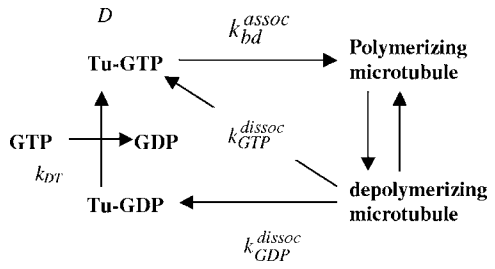

FIG. 1. Schematic representation of the model cycle of MT polymerization. Microtubule growth takes place by addition of solvated Tu-GTP heterodimers to the end of the microtubule with an association rate k_{bd}^{assoc} where the index *bd* denotes a particular site at the tip of a MT (see text for details). In accordance with cap models, Tu-GTP embedded within the lattice of a microtubule, upon further addition of Tu-GTP, hydrolyses to Tu-GDP. A growing microtubule is thus composed of a Tu-GTP cap of newly added Tu-GTP heterodimers and a bulk of Tu-GDP. A microtubule may change its dynamical state between a polymerizing and a depolymerizing state. A depolymerizing microtubule may reject in the solution Tu-GTP heterodimers from its cap as well as Tu-GDP from its bulk. The dissociation rates of these processes are $k_{GTP}^{dissocc}$ and $k_{GDP}^{dissocc}$. GTP in the solution can exchange with liganded GDP to produce Tu-GTP and GDP in solution with a rate k_{DT}. The diffusion coefficient of Tu-GTP is denoted D.

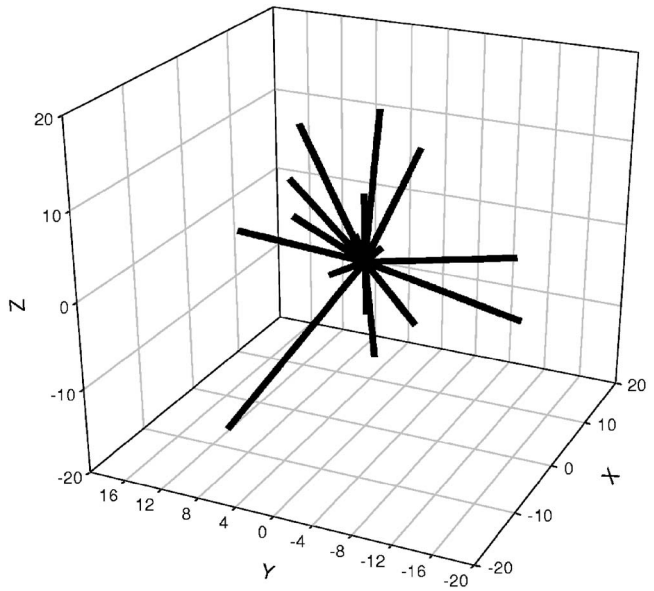

FIG. 2. Schematic illustration of the simulation cell with MT growing from the nucleation center. The axes are in units of $100L_h$ where L_h is the length of a Tu-GTP heterodimer.

disassembly leaves behind a chemical trail of high tubulin concentration, which leads to preferential growth of other MT's in these region. [24–27]. Diffusion was also shown to lead to self-organization in a model of MT's growing in a finite medium and originating from a centrosome [28]. The organization forces are again the tubulin concentration gradients, which are generated by the MT assembly and disassembly. Unfortunately, this later model was limited to only a few microtubules.

The objective of the present paper is to investigate theoretically the effect of free tubulin heterodimer diffusion on the collective growth of MT's nucleated from a centrosomelike nucleation center. Since tubulin dimer diffusion is dependent on the environment in which MT's grow (i.e., slow diffusion is expected in the cell cytoplasm while tubulin will diffuse significantly faster in *in vitro* aqueous solutions), another objective of this work is to demonstrate environment-driven morphological changes in the growth of a collection of MT's. The model and kinetic Monte Carlo method used to study collective MT dynamics including diffusion are described in details in Sec. II. Results are reported and discussed in Sec. III. Finally conclusions concerning the implication of tubulin diffusion on the growth of collections of MT's are drawn in Sec. IV. We also present in Secs. III and IV qualitative comparisons between our predictions and available experimental observations.

II. MODEL AND METHOD

The objective of this work is to shed light on the interplay between Tu-GTP heterodimer diffusion and collective growth of MT's. We consider a reduced model of the cycle of microtubule polymerization (Fig. 1) that retains the essential features and dynamics of MT growth. In this model, MT disassembly is assumed to lead directly to production of Tu-GDP and not to oligomers as intermediate products of depolymerization. The model also assumes that MT's will grow from a predetermined set of MT nuclei, N_n, with the maximum number of MT's, $N_{MT} \leqslant N_n$.

The nuclei are located at the center of a simulation cell with randomly chosen orientation. The initial length of a nucleus is 15 times the length of one Tu-GTP heterodimer—namely, $L_h \sim 8$ nm. The simulation cell is a cubic box with edge length equal to $4000L_h$. Periodic boundary conditions are applied. MT's are treated as rigid linear polymers with only one active end [(+) end], thus mimicking MT's with their (−) capped or embedded in the nucleating center at the origin of the simulation cell (Fig. 2). The positions of the (+) end of MT's, $\mathbf{R}_I$, $I=1,...,N_{\mathrm{MT}}$, are dynamical variables of the model.

We treat the solution as containing an unlimited supply of solvated GTP such that the production of Tu-GTP by exchange of GTP with liganded GDP is only dependent on the overall concentration of Tu-GDP, [Tu-GDP]. The rate constant for this exchange is denoted k_{DT}. In this model [Tu-GDP] is a global concentration and Tu-GDP heterodimers are not followed individually.

Tu-GTP is the diffusing specie, and $N_{\text{Tu-GTP}}$ is the number of Tu-GTP heterodimers in the simulation cell. This number changes dynamically and depends on the initial concentration of the solution but also on the number of Tu-GTP that add to polymerizing MT's as well as the number of Tu-GDP that convert to Tu-GTP. The location of Tu-GTP heterodimers inside the simulation cell is labeled $\mathbf{r}_i$, with $i=1,...,N_{\text{Tu-GTP}}$. The $\mathbf{r}_i$'s are dynamical variables of the model. The diffusion coefficient of Tu-GTP in the solution is D.

Each MT is modeled with a modified version of the five-start helix lattice model of Bayley *et al.* [14]. With this

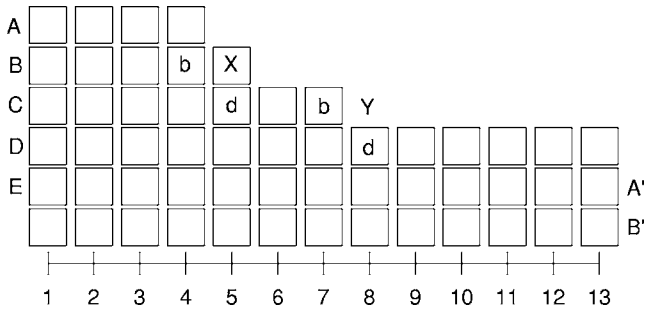

FIG. 3. Schematic illustration of the arrangement of heterodimers at the end of a microtubule with 13-protofilaments. Site A' is contiguous to site A because of helical periodic boundary conditions. X and Y are dissociation and association sites, respectively. Sites b and d, adjacent to X or Y, determine the value of the dissociation or association constants.

model a single MT consists of a two-dimensional helical lattice composed of 13 grid sites (13 tubulin heterodimer protofilaments) perpendicular to the direction of growth (MT principal axis) (see Fig. 3).

The lattice is infinite along the principal direction of the MT. Helical periodic boundary conditions (PBC's) are applied to wrap the lattice into a tubular structure with a helicity of five lattice sites (i.e., sites A and A' in Fig. 3 are contiguous). We employ the standard set of rate constants from the work of Bayley *et al.* The rate constant of association of a Tu-GTP to site Y is dependent on the concentration of Tu-GTP seen by a MT, $[\text{Tu-GTP}]_I$, and is calculated as $k_{bd}^{assoc}[\text{Tu-GTP}]$ where k_{bd}^{assoc} takes on the value 0.33×10^6, $1. \times 10^6$, and 1.25×10^6 mol^{-1} liter s^{-1} when the neighboring sites b and d are both composed of Tu-GDP, a Tu-GTP, and a Tu-GDP, both composed of Tu-GTP, respectively. The dissociation rate constant of a Tu-GDP on site X, k_{GDP}^{dissoc}, is independent of the nature of the neighboring sites b and d and is chosen to be 111.66 s^{-1}. The dissociation rate constant of a Tu-GTP on site X, k_{GTP}^{dissoc}, depends on the type of tubulin dimers present on the neighboring sites and takes on the values 66.66, 8.33, and 1.25 s^{-1} when the sites b and d are both composed of Tu-GDP, a Tu-GTP, and a Tu-GDP or of Tu-GTP, respectively. For the sake of clarity, the reaction rates are illustrated in Fig. 1 along with the relevant processes involved in the dynamics of MT's. Note that in contrast to the model of Bayley *et al.*, here the concentration $[\text{Tu-GTP}]_I$ is a local dynamical variable that depends on the number of Tu-GTP heterodimers in the vicinity of the (+) end of a MT I. This local concentration is calculated from $[\text{Tu-GTP}]_I = 1/N_A V_I$. N_A is the Avogadro number, and V_I is the volume associated with the Tu-GTP heterodimer closest to the tip of the MT I. This volume is obtained from $V_I = \frac{4}{3}\pi(dr_I)^3$ with $dr_I = \min(|\mathbf{R}_I - \mathbf{r}_i|)$, $I = 1, \ldots, N_{\text{Tu-GTP}}$ being the distance between the tip of the MT and the closest Tu-GTP heterodimer. The local concentrations are then rescaled such that their average matches the overall concentration of Tu-GTP in the simulation cell.

The kinetic Monte Carlo (KMC) method is employed to evolve the model dynamically. The steps involved in the KMC simulations are the following.

A. Selection of the event with the shortest time among all possible association and dissociation events at the tip of the MT's:

1. Identify along the jagged helical surface of the tip of the MT's the sites s for dissociation (e.g., site X) and association (e.g., site Y).

2. Calculate the local concentration at the end of each MT, $[\text{Tu-GTP}]_I$.

3. Assign a rate constant k_s for dissociation or association events at every site s. These rate constants depend on the physical structure of the binding site, the nucleotide content of the unit in adjacent protofilaments, and $[\text{Tu-GTP}]_I$ in the case of association.

4. Calculate the time t_s for dissociation or association at every site s at which an event would occur statistically using the relationship $t_s = -\ln(1 - A_s)/k_s$ where A_s is a random number uniformly distributed between 0 and 1.

5. The event with the shortest time (t_{min}) is accepted, and the lattice of that particular MT is modified. For addition events, we implement a hydrolysis rule for conversion of Tu-GTP into Tu-GDP when a Tu-GTP molecule is completely embedded into the MT lattice.

6. The total time is incremented by t_{min}.

B. Update the concentrations of heterodimers:

1. If an association event is selected in A, search for the Tu-GTP closest to the end of the growing MT and eliminate that Tu-GTP from the pool of available Tu-GTP heterodimers—i.e., reduce $N_{\text{Tu-GTP}}$ by 1.

2. If a dissociation event involving a Tu-GTP is selected in A, add a Tu-GTP to the pool of available Tu-GTP's with coordinates equal to those of the end of the MT.

3. If a dissociation event involving a Tu-GDP is selected in A, increase the number of Tu-GDP, $N_{\text{Tu-GDP}}$, as well as the concentration [Tu-GDP].

C. Conversion of Tu-GDP to Tu-GTP:

1. Calculate the number of Tu-GDP that will exchange GDP for GTP during the time t_{min} according to $k_{DT}[\text{Tu-GDP}]t_{min}$.

2. Add the appropriate number of Tu-GTP heterodimers to the pool of Tu-GTP's available for further MT growth. Generate the coordinates of the added Tu-GTP at random.

D. Diffusion:

1. Calculate the diffusion length, $L_d = \sqrt{6Dt_{\text{min}}}$.

2. Implement a random walk of all available Tu-GTP heterodimers by updating the coordinates of the Tu-GTP hetrodimers according to $\mathbf{r}_i(t + t_{\text{min}}) = \mathbf{r}_i(t) + \mathbf{W}L_d$ where $\mathbf{W}$ is a random vector with components varying between -1 and 1.

3. Apply periodic boundary conditions. Any Tu-GTP heterodimer that may exit the simulation cell is brought back inside the cell on the opposite side.

The model conserves the number of tubulin in the system. That is, the sum of the number of tubulin (Tu-GTP and Tu-GDP) in solution and in MT's is a constant. Replacing the local Tu-GTP concentrations $[\text{Tu}-\text{GTP}]_I$ by the uniform overall concentration [Tu-GTP] reduces the model to MT growth in the limit of very fast Tu-GTP heterodimer diffusion (i.e., diffusion-independent growth). The depolymerization of a MT cannot proceed beyond the length of a nucleus. Disassembled MT's that shrink back to the nucleus state are free to initiate the growth of a new MT.

III. RESULTS AND DISCUSSION

In a first series of simulations, we verify the validity of the model in the case of a uniform [Tu-GTP] concentration. That is, every MT experiences the same tubulin concentration at its plus end. This concentration is calculated as the overall Tu-GTP concentration. This model is comparable to mean-field models previously reported in the literature [17–22]. A major difference is that we do not allow complete disassembly of the nuclei or formation of additional nuclei. The number of nuclei, N_n, is fixed to a value of 100. We have considered two initial [Tu-GTP] concentrations of 25×10^{-5} and 60×10^{-5} mol.

Figure 4 shows the evolution of the average length of the MT's as a function of time for several values of k_{DT}, the rate constant for exchange of Tu-GDP to Tu-GTP. The results presented are limited to short periods of time. In accord with Ref. [19], as k_{DT} increases at fixed initial composition, the collective growth of MT's evolves from damped oscillations and stabilization at a short average length (small k_{DT}) to nearly sustained oscillations (intermediate k_{DT}) to damped oscillations and stabilization at a long average length (large k_{DT}). The period of oscillations in our simulations is on the order of 10 s, which is smaller by a factor of approximately 10 than that reported by other authors [19,22]. This difference is essentially due to the choice of rate constants in our kinetic Monte Carlo model. The oscillation time can be matched simply by rescaling the rate constants. In Fig. 5, we report the time evolution of the length of all 100 seeded MT's with homogeneous [Tu-GTP]. Initially, all the MT's grow synchronously due to an ample supply of Tu-GTP. Once [Tu-GTP] decreases below the critical concentrations ($C_c\sim9\times10^{-6}$ mol), we observe a differentiation of the population of MT's. A significant fraction of the MT's depolymerizes rapidly, leading to a decrease in average length before GDP to GTP exchange supplies the solution in fresh Tu-GTP, initiating growth recovery. The synchronicity of these events is lost after several cycles. The growth of MT's is bounded, and the stochasticity of dynamic instability ensures that no single microtubule grows indefinitely. The MT's undergo rapid dynamics involving successive periods of growth and disassembly. The growth velocity of a MT is approximately 1.5 μm/min, and the disassembly velocity approximately 10 times faster. At steady state, the MT's take on an aster morphology with a population distribution decreasing monotonously from short to long MT. The synchronization of the MT oscillations is permitted by the homogeneity of the tubulin concentration that overcomes the spatial separation between MT ends. In reality, the diffusion length of tubulin is finite and spatial inhomogeneities should lead to dephasing and morphological changes in the MT growth. The results of Fig. 5 represent the behavior of MT's grown from a nucleation center in the limit of fast diffusion. The effect of diffusion on MT growth is reported and discussed below as well as compared to the observations of Fig. 5.

A second series of simulations is then conducted to shed light on the effect of tubulin diffusion on MT collective growth. In all these simulations $N_n=100$ and $k_{DT}=0.5$. We estimate the diffusion coefficient of a tubulin dimer in water by using the Stokes-Einstein relation: namely,

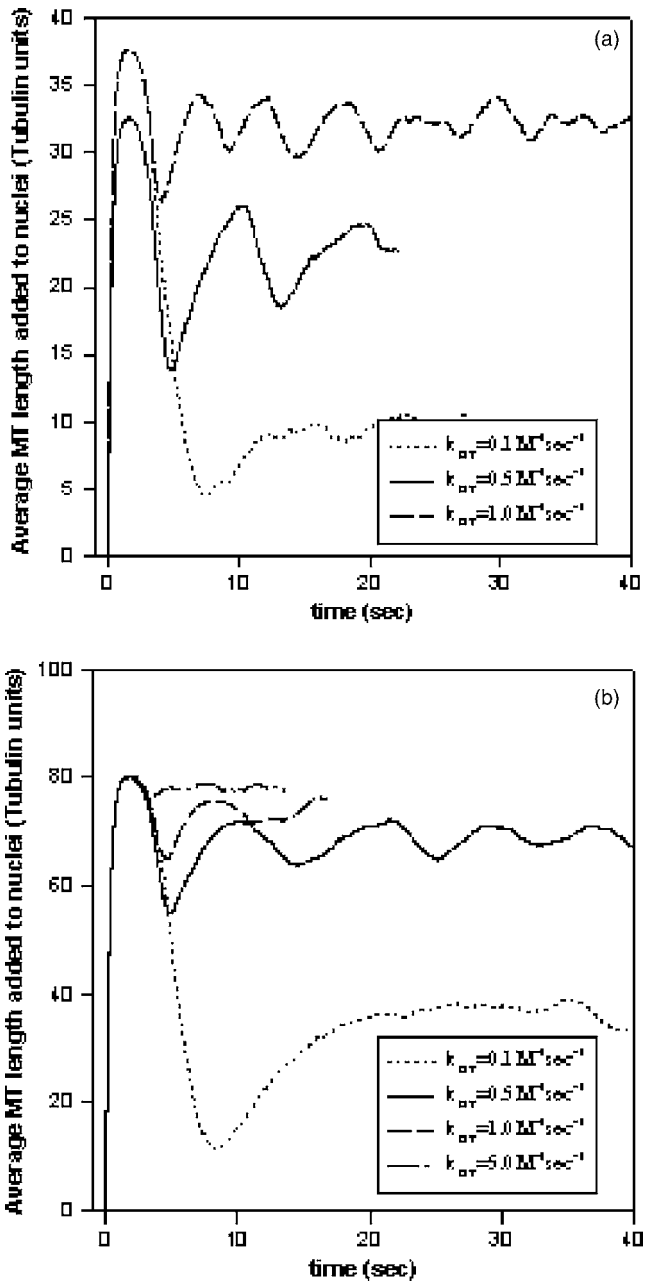

FIG. 4. Time evolution of the average length added to MT seeds for several GTP-GDP exchange rates. The concentration of Tu-GTP is homogeneous in these simulations. The number of nuclei is 100 and the initial Tu-GTP concentrations are (a) 25×10^{-5} mol and (b) 60×10^{-5} mol.

$D=k_BT/6\pi R\eta$ where k_B is Boltzmann's constant, T the temperature, R the radius of the diffusing particle, and η the viscosity of the fluid ($\eta_{\text{water}}=10^{-3}$ Pa s^{-1}). Tubulin dimers are cylindrical in shape with a length of $\sim$8 nm and a diameter of $\sim$4 nm [7]. Inserting into the preceding relation two possible lengths or radii corresponding to diffusion along or across the dimer axis, $R=4$ and 2 nm, results in values for the diffusion coefficients in water at $T=300$ K of $D=5.5\times10^{-11}$ m^2 s^{-1} and $D=11\times10^{-11}$ m^2 s^{-1}. On the another hand, diffusion of Tu-GTP *in vivo* is expected to be significantly slower. *In vivo* measurements of the diffusion coeffi-

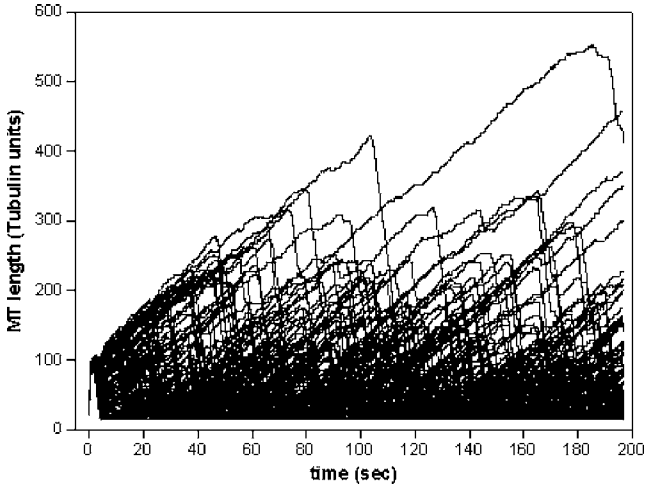

FIG. 5. Length of 100 seeded microtubules as a function of time. The [Tu-GTP] is homogeneous with an initial value of 60×10^{-5} mol and $k_{DT}=0.5$.

cient of tubulin yielded $D\sim0.6\times10^{-11}$ m^2 s^{-1} [29]. As a consequence, we vary the diffusion coefficient in our simulations over a wide range of values: namely, [0.1–100] $\times10^{-11}$ m^2 s^{-1}, which includes the estimated diffusion coefficient of tubulin in water, but also diffusion in other environments with higher viscosity such as for instance the cytoplasm.

The dynamics of the MT's length for initial Tu-GTP concentrations of 25 and 60×10^{-5} mol and three values of the Tu-GTP diffusion coefficient is presented in Figs. 6 and 7. The short-time behavior is similar to that of the homogeneous Tu-GTP simulations with all MT's growing in phase. However, the growth rapidly loses synchronicity after the first collective dissociation and first recovery of a fraction of the MT's (see Fig. 8). The system exhibits very different long-time behavior depending on the value of D. For small values of the diffusion coefficients, the MT's divide into two subpopulations. One subpopulation corresponds to MT's undergoing bounded growth. These MT's have nearly completely depolymerized and have lengths that have collapsed back to the dimensions of the nucleus. These MT's are all located at the core of the nucleation center and compete with each other for the few Tu-GTP dimers that may diffuse inside their interaction volume. The slow diffusion coefficient and the competition for tubulin dimers inhibit further growth of these MT's. On the other hand, MT's that have successfully grown outside the volume of interaction of the nucleation center constitute the second subpopulation. These MT's appear to grow unbounded and independently of each other as they forage the random field of slowly diffusing tubulin dimers. Their length is narrowly distributed. The three diffusion coefficients 0.1, 1, and 100×10^{-11} m^2 s^{-1} result in an estimated average growth velocity of the unbounded MT's of 0.1, 0.4, and 2.9 μm/min and 0.2, 0.5, and 4.5 μm/min for initial Tu-GTP concentrations of 25×10^{-5} and 60×10^{-5} mol, respectively. The very slow growth velocity of unbounded MT's for small values of the diffusion coefficient is indicative of the stability of these MT's. At times, some of the MT's in the second subpopulation undergo random catastrophic depolymerization and collapse into the nucleation center in which they become trapped. The small diffusion coefficient, therefore, induces a decoupling between different regions of space and leads to a morphological evolution of the long-time MT population distribution toward a bimodal distribution corresponding to short MT's in the nucleation center and long MT's outside the nucleation center. Although our model geometry represents MT growth from a centrosome like nucleation center, our results are qualitatively consistent with the theoretical results of Dogterom and Leibler [23] for a semi-infinite geometry model of the growth of MT's from a substrate combining also reaction dynamics and diffusion. That study shows the existence of a transition between bounded and unbounded growth with MT's undergoing unbounded growth, creating a region of tubulin depletion in the vicinity of the surface. These authors observe that as the concentration in the depletion region, decreases below the critical concentration, further growth is inhibited in that region, leading to the creation of two subpopulations of MT: short MT's undergoing assembly and dis-

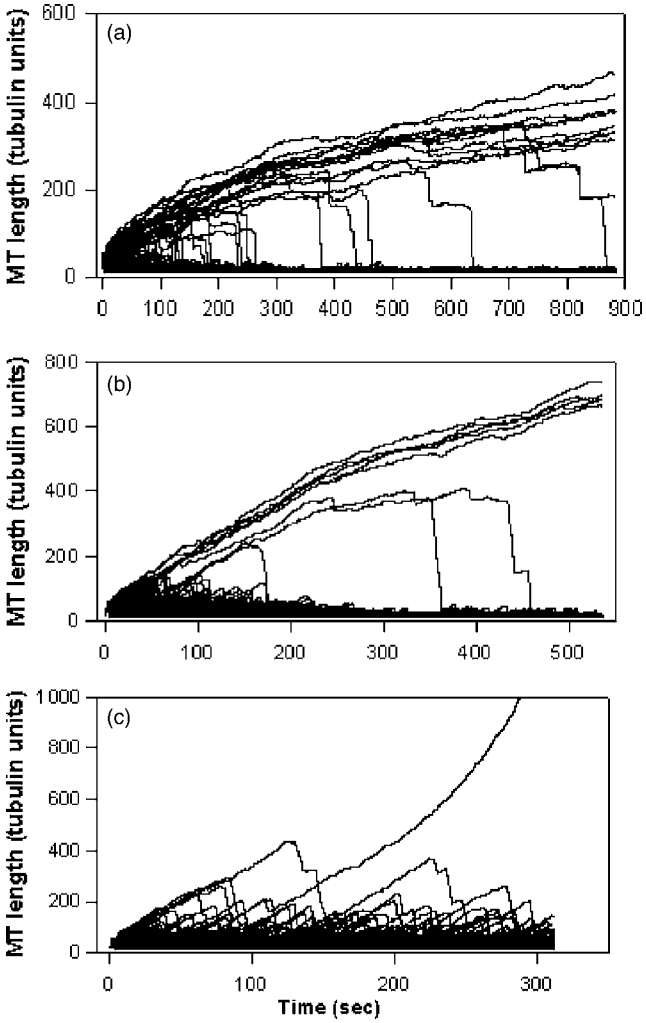

FIG. 6. Time evolution of the length of 100 MT's. $[\text{Tu–GTP}]_{\text{initial}}=25\times10^{-5}$ mol. The tubulin diffusion coefficient D is equal to (a) 0.1×10^{-11} m^2 s^{-1}, (b) 1.0×10^{-11} m^2 s^{-1}, and (c) 100×10^{-11} m^2 s^{-1}.

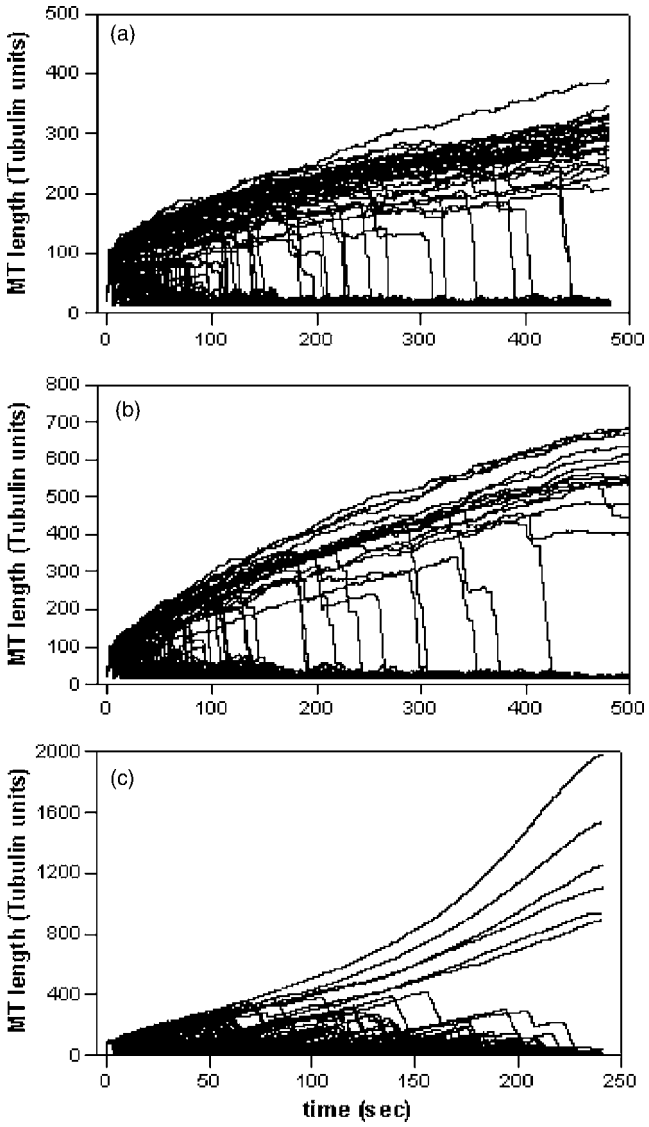

FIG. 7. Time evolution of the length of 100 MT's. $[\mathrm{Tu-GTP}]_{\mathrm{initial}}=60\times10^{-5}$ Mol. The tubulin diffusion coefficient is equal to (a) 0.1×10^{-11} m^2 s^{-1}, (b) 1.0×10^{-11} m^2 s^{-1}, and (c) 100×10^{-11} m^2 s^{-1}.

assembly near the surface and a "packet" of unbounded MT's growing beyond the depletion region.

For a given value of the diffusion coefficient, we observe a smaller number of unbounded MT's for the lower initial concentration. This result is in accordance with Ref. [23] where the number of MT's that have escaped the depletion region approaches zero as the initial concentration approaches the critical concentration. We observe, however, that the number of MT's in the unbounded subpopulation decreases as the diffusion coefficient (i.e., the diffusion length) increases. For larger D, the majority of MT's belong to the first subpopulation and their overall behavior resembles that of the simulations with uniform tubulin concentration, with MT's undergoing rapid assembly and disassembly with growth velocities comparable to those of Fig. 5. As the diffusion coefficient increases, the bounded MT's are also able to grow to lengths significantly longer than in the

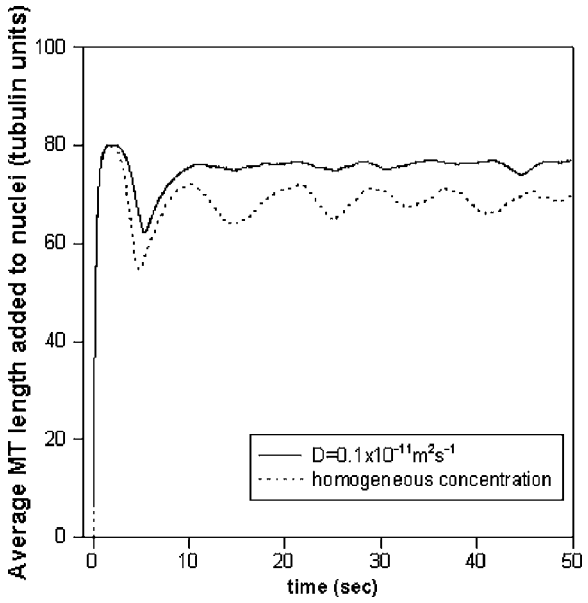

FIG. 8. Early-time dependence of the average MT length in the case of a homogeneous tubulin concentration and inhomogeneous concentration (small diffusion coefficient). The initial tubulin concentration is 60×10^{-5} mol and the GTP/GDP exchange rate is 0.5 mol^{-1} s^{-1}.

case of slow diffusion before they undergo disassembly.

To analyze the behavior of the unbounded MT's, we define a length L over which tubulin dimers diffuse before a dimer reacts with the tip of a MT. The square of that length is given by $L^2\sim D/r$ where the rate of attachment of a tubulin at the tip of a MT, r, can be estimated from the growth velocity of a MT at the two initial concentrations studied. The growth velocity is dependent on the tubulin concentration. From the initial growth spur of Figs. 6 and 7, we calculate an average initial MT growth velocity of ~85 μm/min and 40 μm/min for the initial concentrations of 60×10^{-5} and 25×10^{-5} mol, respectively. With MT's constituted of 13 protofilaments and a tubulin dimer length of 8 nm, the MT growth velocities convert to the rates of tubulin attachment to the MT tip of ~13.6 and 6.4 s^{-1} for the high and low initial tubulin concentrations. The three diffusion coefficients of 0.1, 1, and 100×10^{-11} m^2 s^{-1} yield $L\sim0.3$, 0.9, and 8.6 μm for the tubulin concentration of 60×10^{-5} mol and $L\sim0.4$, 1.2 and 12.5 μm at the lower concentration of 25×10^{-5} mol. After the transient time when subpopulations of bounded and unbounded MT's differentiate, the Tu-GTP concentration of the solution is oscillating about the critical concentration and most of the initial tubulin dimers are incorporated into the unbounded MT's. To estimate the number of unbounded MT's we make the assumption that differentiation between the two subpopulations of MT's occurs when the unbounded MT's have reached a length equal to L. This choice is reasonable considering that under this condition, free Tu-GTP is not able to diffuse inside the nucleation center before being captured by an unbounded MT. The number of unbounded MT's should scale with the initial number of tubulin proteins and the length L as $N_u\sim N_{Tu\text{-}GTP}^{initial}L_h/(13L)$. The number of unbounded MT's,

therefore, scales as the inverse of the square root of the diffusion coefficient and the square root of the rate of attachment of Tu-GTP as $N_u \sim N_{Tu\text{-}GTP}^{initial}(L_h/13)\sqrt{r/D}$. We have verified that the long-time limit of the number of unbounded MT's scales reasonably well according to the previous equation considering the limited data. In summary, the transition from unbounded to bounded growth appears to be consistent with a mechanism driven by the competition between reaction rate of tubulin assembly and the diffusion rate of free tubulin.

IV. CONCLUSIONS

We have introduced a kinetic Monte Carlo model of MT dynamics that can account for the diffusion of tubulin heterodimers. In the absence of a diffusion limit (i.e., under conditions of uniformity of the Tu-GTP concentration), the growth of MT's is synchronous and bounded and our model agrees qualitatively with other mean-field models; we observe short-time synchronous oscillations. MT's growing from a nucleation center form an aster with a long-time monotonously decreasing length distribution. We show that accounting for tubulin diffusion leads to rapid dephasing in the MT growth dynamics, unbounded growth of some MT's, spatial inhomogeneities, and morphological change. The very-short-time behavior is similar to that of the simulations with uniform [Tu-GTP]. In contrast, the long-time behavior leads to an organization of the MT's in an aster morphology with bimodal length distribution. The center of the aster (i.e., nucleation center) is composed of competing short bounded MT's. The aster is also composed of long unbounded MT's growing slowly and monotonously with narrowly distributed lengths. Our simulations show therefore a strong effect of tubulin diffusion on MT morphology. In support of our theoretical observation, diffusion was shown experimentally to impact MT self-organization. Experimentally, the contribution of diffusion to MT self-organization was demonstrated by carrying MT assembly in gels that inhibit diffusion [30–32].

In order to compare our simulation results with morphological changes of MT's nucleated from centrosomes in cellular systems, we note that living cells will not vary the diffusion rate as readily as the rate of tubulin reactions. However, we have shown that the number of long unbounded MT's in our model depends on the ratio of the attachment rate of tubulin to the diffusion coefficient. This observation suggests that control of the morphology of MT growing from a centrosome can be achieved not only by varying the diffusion coefficient at a fixed reaction rate but also by regulating the reaction rates of tubulin assembly and disassembly at a fixed diffusion coefficient value. Therefore, regulation of the various parameters of dynamic instability (reaction rates) and not diffusion is likely to be the determinant factor in controlling the morphology of MT's in living cells. Numerous proteins and molecules regulate MT polymerization [33]: for instance, microtubule-associated proteins (MAP's) are known to stabilize MT's. MT regulating agents have been shown to lead to MT morphological and dynamical changes of MT's [34,35]. For instance, MT's nucleated from centrosomes extracted from Xenopus eggs undergo a transition similar to the one reported in our study [35]. Interphase extracts show MT asters composed of slow growing or shrinking very long MT's while asters in extracts driven into mitosis by addition of cyclin protein contain only short MT undergoing rapid dynamics. While our study shows the effect of the tubulin diffusion coefficient on an unbounded to bounded MT growth transition, the results of the simulations are qualitatively comparable to the morphological and dynamical changes of centrosome-nucleated MT's from interphase to mitosis in cellular systems where the transition is regulated by the reaction rates of tubulin assembly and disassembly.

ACKNOWLEDGMENTS

We acknowledge financial support from the National Science Foundation, NIRT Grant No. 0303863.

[1] R. H. Wade and A. A. Hyman, Curr. Opin. Cell Biol. **9**, 12 (1997).
[2] B. Alberts, D. Bray, J. Lewis, M. Raff, K. Roberts, and J. D. Watson, *Molecular Biology of the Cell* (Garland, New York, 1994), Chap. 16.
[3] S. C. Schuyler and D. Pellman, Cell **18**, 421 (2001).
[4] Y. F. Inclan and E. Nogales, J. Cell. Sci. **114**, 413 (2000).
[5] P. G. McKean, S. Vaughan, and K. Gull, J. Cell. Sci. **114**, 2724 (2001).
[6] T. Mitchison and M. Kirschner, Nature (London) **312**, 237 (1984).
[7] H. Lodish, A. Berk, S. L. Zipuski, P. Matsudaira, D. Baltimore, and J. Darnell, *Molecular Cell Biology*, 4th ed. (Freeman, San Fransisco, 2000).
[8] T. L. Hill and M. F. Carlier, Proc. Natl. Acad. Sci. U.S.A. **80**, 7234 (1983).
[9] T. L. Hill and Y. Chen, Proc. Natl. Acad. Sci. U.S.A. **81**, 5772 (1984).
[10] M. F. Carlier, T. L. Hill, and Y. Chen, Proc. Natl. Acad. Sci. U.S.A. **81**, 771 (1984).
[11] Y. Chen and T. L. Hill, Proc. Natl. Acad. Sci. U.S.A. **82**, 1131 (1985).
[12] T. L. Hill, Proc. Natl. Acad. Sci. U.S.A. **82**, 431 (1985).
[13] P. Bayley, M. Schilstra, and S. Martin, FEBS Lett. **259**, 181 (1989).
[14] P. M. Bayley, M. J. Schilstra, and S. R. Martin, J. Cell. Sci. **95**, 33 (1990).
[15] S. R. Martin, M. J. Schilstra, and P. M. Bayley, Biophys. J. **65**, 578 (1993).
[16] Y C Tao and C. S. Peskin, Biophys. J. **75**, 1529 (1998).
[17] M. F. Carlier, R. Melki, D. Pantaloni, T. L. Hill, and Y. Chen, Proc. Natl. Acad. Sci. U.S.A. **84**, 5257 (1987).

[18] Y. Chen and T. L. Hill, Proc. Natl. Acad. Sci. U.S.A. **84**, 8419 (1987).
[19] B. Houchmandzadeh and M. Vallade, Phys. Rev. E **53**, 6320 (1996).
[20] E. Jobs, D. E. Wolf, and H. Flyvbjerg, Phys. Rev. Lett. **79**, 519 (1997).
[21] M. Hammele and W. Zimmermann, Phys. Rev. E **67**, 021903 (2003).
[22] A. Marx and E. Mandelkow, Eur. Biophys. J. **22**, 405 (1994).
[23] M. Dogterom and S. Leibler, Phys. Rev. Lett. **70**, 1347 (1993).
[24] N. Glade, J. Demongeot, and J. Tabony, C. R. Biol. **325**, 283 (2002).
[25] J. Tabony, N. Glade, J. Demongeot, and C. Papaseit, Langmuir **18**, 7196 (2002).
[26] J. Tabony and D. Job, Nature (London) **346**, 448 (1990).
[27] C. Papaseit, L. Vuillard, and J. Tabony, Biophys. Chem. **79**, 33 (1999).
[28] C. Robert, M. Bouchiba, R. L. Margolis, and D. Job, Biol. Cell **68**, 177 (1990).
[29] E. D. Salmon, W. H. Saxton, R. J. Leslie, H. L. Karow, and J. R. Mc Intosh, J. Cell Biol. **99**, 2157 (1984).
[30] J. Tabony, Nanobiology **4**, 117 (1996).
[31] J. Tabony and C. Papaseit, Adv. Struct. Biol. **5**, 43 (1998).
[32] J. Tabony, L. Vuillard, and C. Papaseit, Adv. Complex Syst. **2**, 221 (2000).
[33] A. Desai and T. J. Mitchison, Annu. Rev. Cell Dev. Biol. **13**, 83 (1997).
[34] N. R. Glickman, S. F. Parsons, and E. D. Salmon, J. Cell Biol. **119**, 1271 (1992).
[35] L. D. Belmont, A. A. Hyman, K. E. Sawin, and T. J. Mitchison, Cell **62**, 579 (1990).